

1 Optimizing Walktrap's Community Detection in Networks Using the Total Entropy Fit Index

2 Laura Jamison<sup>1</sup>, Hudson F. Golino<sup>1</sup>, & Alexander P. Christensen<sup>2</sup>

3 <sup>1</sup> University of Virginia

4 <sup>2</sup> University of Pennsylvania

5 Author Note

6 Add complete departmental affiliations for each author here. Each new line herein  
7 must be indented, like this line.

8 Enter author note here.

9 Correspondence concerning this article should be addressed to Laura Jamison, Postal  
10 address. E-mail: [lj5yn@virginia.edu](mailto:lj5yn@virginia.edu)

## Abstract

11

12 *Exploratory graph analysis* (EGA) is used to estimate the structural organization of  
13 variables, uncovering latent dimensions as clusters of nodes. EGA first estimates a weighted  
14 network then uses the Walktrap algorithm to detect clusters of nodes. The Walktrap  
15 algorithm uses random walks to estimate the topography of a graph. The number of random  
16 walks taken ( $t$ ) is typically set statically. However, the impact of  $t$  and the properties  
17 determining its optimization have yet to be fully researched. The present study proposes and  
18 tests a new approach optimizing  $t$  by iteratively varying  $t$  and employ *total entropy fit index*  
19 as a fit index to identify the number of steps that best fit the data using a Monte-Carlo  
20 simulation varying data structure characteristics. Results indicate that the proposed method  
21 is most effective for a higher number of variables per factor and when variables are  
22 polytomous. Varying  $t$  is important as spurious connections are introduced between  
23 communities. An empirical example using the Developmental Coordination Disorder  
24 Questionnaire is shown demonstrating improved measure interpretation by optimizing the  
25 Walktrap algorithm. The paper finishes with a discussion about the relevance of the findings  
26 and future directions for research.

27

*Keywords:* keywords

28

Word count: X

29 Optimizing Walktrap’s Community Detection in Networks Using the Total Entropy Fit Index

30

## Introduction

31 Within psychological research, network modeling approaches have been steadily  
32 gaining popularity across clinical psychology (Borsboom, 2017; McNally, 2016),  
33 developmental psychology (Dijkstra, Cillessen, & Borch, 2013), psychopathology (Bringmann  
34 et al., 2013), and in particular, psychometrics (Costantini et al., 2019; Golino, Shi, et al.,  
35 2020; Marsman et al., 2018). Within network psychometrics, a common goal of research is to  
36 estimate the structural organization of variables (e.g., items in a survey or test) by  
37 uncovering latent dimensions as clusters of nodes in weighted networks, a general approach  
38 termed *exploratory graph analysis* (**EGA**; Golino & Epskamp, 2017; Christensen et al.,  
39 2019b, 2019c; Golino, Shi, et al., 2020). EGA is an innovative approach for dimensionality  
40 assessment and reduction that starts by estimating a network (Golino, Shi, et al., 2020) and  
41 then uses the Walktrap algorithm (Pons & Latapy, 2006) to detect clusters of nodes.

42 The Walktrap algorithm is a modularity-based approach (similar to cluster analysis),  
43 shown to outperform other algorithms (e.g., Fast Greedy, Newman’s Spectral Approach)  
44 when using correlation matrices and sparse count networks (Christensen, Garrido, & Golino,  
45 2021; Gates, Henry, Steinley, & Fair, 2016; Orman & Labatut, 2009) and has been repeatedly  
46 found to successfully uncover community structure in both small and large networks (Golino,  
47 Shi, et al., 2020; Pons & Latapy, 2006; Yang, Algesheimer, & Tessone, 2016). In the area of  
48 dimensionality analysis and reduction, when EGA is used with the Walktrap algorithm, it  
49 has shown to perform above and beyond other methods used in factor analysis when the  
50 data generating mechanism is a factor model (Golino & Epskamp, 2017). These findings  
51 make the Walktrap algorithm an attractive choice for substantive psychological research,  
52 from neuroscience (Gates et al., 2016) to the study of individual differences (Golino, Shi, et  
53 al., 2020).

54 The Walktrap algorithm has been used in many applications in psychology. For  
55 example, the group iterative multilevel model estimation (*GIMME*) uses the Walktrap  
56 algorithm as a part of a process designed to recover connections and directionality within  
57 regions of interest from fMRI data (Gates & Molenaar, 2012). Another method focuses on  
58 detecting communities within networks using Cohen’s  $\kappa$  for clustering social network data  
59 (Hoffman, Steinley, Gates, Prinstein, & Brusco, 2018), while EGA aims to estimate the  
60 number of dimensions in multivariate data (Golino & Epskamp, 2017; Golino, Shi, et al.,  
61 2020). In each application, the Walktrap algorithm uses a series of random walks to define  
62 one important characteristic of the topography of a graph: the number and composition of  
63 communities (i.e., clusters of nodes or variables). The algorithm begins with a square matrix,  
64 the values of which indicate the relationship between units of analysis. In psychology, this  
65 matrix is typically made up of (partial) correlations between variables which form weighted,  
66 undirected graphs when modeled using network techniques.

67 A network is considered to have a good community structure when the average edge  
68 weight within a community is higher than the edge weights between that community’s nodes  
69 and nodes in other communities (Newman, 2006; Pons & Latapy, 2006). The Walktrap  
70 algorithm capitalizes directly on this definition of good community structure by using a  
71 series of random walks. Starting in a given node, the algorithm repeatedly moves along the  
72 edges connecting that node to its neighbors. A probability function determines where it is  
73 more likely to “walk” to a node with a higher degree than a node with a lesser degree. In  
74 this way, the process will get “trapped” within a community because it is less probable for it  
75 to move to a node that does not belong in that community.

76 The number of random walks ( $t$ ) taken is generally set statically as an empirical  
77 compromise to computational efficiency to make sure algorithm run time is reasonable (Pons  
78 & Latapy, 2006). Pons and Latapy (2006) recommend taking steps  $t = 4$  or  $t = 5$  as the  
79 most computationally efficient approach with the least empirical compromise. Typically, a

80 random walk of  $t = 4$  is used in many applications (Gates et al., 2019; Golino, Shi, et al.,  
81 2020). Pons and Latapy (2006) state that  $t$  must be large enough to adequately capture the  
82 topography of the graph, but if  $t$  is too large, then the probability of transitioning from one  
83 node to another depends solely on the degree of the second node. As sparsity increases,  $t$  can  
84 also increase as the convergence speed of the algorithm increases, and conversely  $t$  should  
85 decrease as density increases (Pons & Latapy, 2006). However, the impact of  $t$  and the  
86 properties determining its optimization have yet to be fully researched. This is especially  
87 pressing in the network psychometric literature which uses a range of data structures from  
88 many subfields of psychology, thus making a “one solution fits all” approach unlikely.

89 The goal of the current paper is to propose and test a new approach to optimize the  
90 number of steps of the Walktrap algorithm, which could potentially improve its accuracy to  
91 identify groups of variables in weighted networks. Instead of using a predetermined number  
92 of steps, we iteratively vary the number of steps (from 3 to 10) and employ a novel fit index  
93 termed *total entropy fit index* (**TEFI**; Golino, Moulder, et al., 2020) to identify the number  
94 of steps that best fit the data. A Monte-Carlo simulation is implemented to verify if our  
95 optimization approach improves the capacity of the Walktrap algorithm to estimate the  
96 number of factors (clusters of nodes) in weighted networks. We controlled several important  
97 characteristics: sample size, number of variables per factor, factor loadings, interfactor  
98 correlation, type of variable, link probability, type of correlation and network estimation  
99 method. The paper is organized as follows: first we will present a general overview of  
100 network model estimation used in this study followed by an in depth review of the Walktrap  
101 algorithm. Then, we will discuss the proposed method as well as the methods and metrics  
102 used to test it. Finally, an empirical example is shown to demonstrate how our optimization  
103 approach improves the interpretation of the final partition of the network into distinct  
104 communities or factors using data from the Developmental Coordination Disorder  
105 Questionnaire (DCDQ; Schoemaker et al., 2006).

## 106 Estimating Factors in Network Psychometrics

107 **Network Model Estimation.** To estimate the number and composition of factors  
108 in the network psychometrics literature, EGA is used. EGA uses two main network  
109 estimation methods: the graphical least absolute shrinkage and selection operator (glasso;  
110 Friedman, Hastie, & Tibshirani, 2008) and triangulated maximally filtered graph (TMFG;  
111 Massara, Di Matteo, & Aste, 2016).

112 The *glasso* is a commonly used method for estimating networks that are known as  
113 Gaussian Graphical Models (GGM) (Lauritzen, 1996). The original input matrix and the  
114 edges of the network are made up of partial correlations between variables, in other words  
115 the correlation between variables after conditioning on all other variables in the network.  
116 The lasso operator shrinks coefficients to zero (to account for spurious relationships and  
117 control for overfitting to the data). This creates a sparse network that can be formed at  
118 different levels between a completely connected network to an entirely unconnected network.  
119 As each network in this range is estimated, the extended Bayesian information criterion  
120 (EBIC) (Chen & Chen, 2012) is computed. The network with the lowest EBIC is selected  
121 (Epskamp et al., 2018, 2018; Foygel & Drton, 2010). The EBIC has a hyperparameter that  
122 provides a penalization for more complicated models to help control for overfitting to the  
123 data (Epskamp & Fried, 2018). Typically, this hyperparameter ( $\gamma$ ) is set to 0.5 (Foygel &  
124 Drton, 2010). Lower values of  $\gamma$  provide greater sensitivity but may reduce specificity  
125 (Williams, Rhemtulla, Wysocki, & Rast, 2019). As such, EGA starts off using  $\gamma = 0.5$ . If the  
126 network has disconnected nodes, EGA will continue to lower the value of  $\gamma$  until this is no  
127 longer the case.

128 The TMFG algorithm is another commonly used method for network estimation that  
129 works by constraining the number of zero-order correlations included in the network to be  
130  $3n - 6$ , where  $n$  is the number of variables (Christensen et al., 2019a; Golino, Shi, et al.,

131 2020; Massara et al., 2016). The algorithm begins by connecting together the four variables  
132 that have the highest correlation sum to all other variables. Iteratively, variables are added  
133 to this network based on the highest correlation sum of three variables with nodes already  
134 contained in the network.

135 **Walktrap Algorithm.** After estimating a weighted network, the EGA technique  
136 uses the Walktrap algorithm to uncover the number and composition of latent factors,  
137 represented in networks as clusters of densely connected nodes (Golino, Shi, et al., 2020).  
138 The Walktrap algorithm (Pons & Latapy, 2006) transforms the original correlation matrix  
139 into a matrix containing transition probabilities called a transition matrix. Transition  
140 probabilities refer to the probability of transitioning between nodes based on edge strength.  
141 Edge strength is defined by the strength of the relationship between nodes, in this case the  
142 partial correlation between variables. This is done using a series random walks, typically of  
143 length 4, to estimate a distance measure for each pair of nodes. The algorithm then seeks to  
144 minimize the sum of squared distances between each node and all other nodes in its cluster  
145 using Ward’s hierarchical clustering method (Ward Jr, 1963).

146 More formally, the Walktrap algorithm begins with a weighted, undirected original  
147 input matrix,  $A$ , where  $A_{ij}$  is the strength between node  $i$  and node  $j$ . The algorithm  
148 reconstructs matrix  $A$  into a transition matrix,  $P$ , using a Markov chain random walk  
149 process defining the transition probability between node  $i$  and node  $j$  to be  $P_{ij} = \frac{A_{ij}}{d(i)}$  and  
150 doing so in length  $t$  to be  $P_{ij}^t$ . Note that this probability will be influenced by the degree  
151 (number of connections) of node  $j$  such that there is a higher probability of transitioning to a  
152 node with a higher degree.  $P_{ij}^t$  will also be higher when  $i$  and  $j$  are in the same community,  
153 however a high  $P_{ij}^t$  does not necessarily mean that nodes  $i$  and  $j$  are in the same community.  
154 Using random walks, a distance  $d$  will be defined between nodes.

$$d_{ij} = \sqrt{\sum_{k=1}^n \frac{(P_{ik} - P_{jk})^2}{NS(k)}} \quad (1)$$

155 Where  $k$  refers to the cluster node  $i$  and  $j$  belong to.  $r$  should be smaller between node  
 156  $i$  and node  $j$  if they are in the same community and comparatively larger if they are not in  
 157 the same community. This same logic can be applied to define the distance between node  $j$   
 158 and community  $C$  by

$$P_{Cj}^t = \frac{1}{|C|} \sum_{i \in C} P_{ij}^t \quad (2)$$

159 We can then define the distance between communities  $C_1$  and  $C_2$  to be

$$r_{C_1 C_2} = \sqrt{\sum_{k=1}^n \frac{(P_{C_1 k}^t - P_{C_2 k}^t)^2}{d(k)}} \quad (3)$$

160 The Walktrap algorithm uses an agglomerative clustering approach beginning by  
 161 defining the most general case where each node is its own cluster. The distance,  $r$ , is  
 162 computed between each of the nodes. The algorithm then begins to iteratively merge nodes  
 163 with edges between them into larger clusters. Per methodology proposed by Pons and  
 164 Latapy (2006), this merging is done in such a way to approximately minimize the variation  
 165 in squared distances between each node and its community ( $\sigma$ ).

$$\Delta\sigma(C_1, C_2) = \frac{1}{n} \left( \sum_{i \in C_3} r_{iC_3}^2 - \sum_{i \in C_1} r_{iC_1}^2 - \sum_{i \in C_2} r_{iC_2}^2 \right) \quad (4)$$

166 Where  $C_1$  and  $C_2$  are clusters being merged to form a third cluster,  $C_3$ . The resulting  
 167 values will be stored in a dendrogram. From the probabilities given in  $P_{ij}^t$ , the length  $t$  of the  
 168 random walks should be optimized to gather sufficient information to accurately partition



169 the clusters.

## 170 **Optimizing the number of steps in the Walktrap algorithm**

171 As previously stated, the number of random walks ( $t$ ) used in the Walktrap algorithm  
172 is generally set statically as an empirical compromise to computational efficiency, with  $t = 4$   
173 or  $t = 5$  being recommended as the most computationally efficient approach (Pons & Latapy,  
174 2006). In the network psychometrics literature, setting the number of steps as  $t = 4$  has  
175 shown to be effective in recovering the number of simulated factors (Golino, Shi, et al., 2020)  
176 or communities of sparse count data (Gates et al., 2019). As Pons and Latapy (2006) states,  
177  $t$  must be large enough to adequately capture the topography of the graph, but if  $t$  is too  
178 large, then the probability of transitioning from one node to another depends solely on the  
179 degree of the second node. For most applications in psychology in which the Walktrap  
180 algorithm is used to identify communities of densely connected nodes representing latent  
181 factors, as in the EGA approach, tuning the number of steps is highly desirable, since it can  
182 lead to improved factor estimation and can facilitate the interpretation of the factors due to  
183 a improved placement of variables per factor.

184 To tune the Walktrap hyperparameter (i.e. number of steps), we propose an iterative  
185 algorithm. First, a network is estimated (e.g., using the glasso or the TMFG network  
186 methods). Then, the Walktrap algorithm is applied with the number of steps set as 3. The  
187 fit of the resulting partition of the multidimensional space (in this case the partition of the  
188 network into communities) to the data is then computed using the *total entropy fit index*  
189 (**TEFI**: Golino, Moulder, et al., 2020). The TEFI index has shown to present the highest  
190 accuracy in detecting the correct dimensionality solution (i.e. number of factors and correct  
191 placement of variables per factor) in a Monte-Carlo simulation study (Golino, Moulder, et  
192 al., 2020) where traditional fit indices used in factor analysis and structural equation  
193 modeling were also used. The TEFI index assesses the degree of uncertainty of the partition

194 of a multidimensional space into separate distinct categories (i.e., latent factors or clusters),  
 195 where lower TEFI values indicate less uncertainty of the dimensionality solution. In other  
 196 words, lower TEFI values indicates that a given dimensionality structure fits the data better  
 197 than an alternative dimensionality solution with higher TEFI values, indicating that the  
 198 former is more likely to represent the best organization of the variables than the latter. The  
 199 TEFI index is calculated as follows:

$$TEFI = \left[ \frac{\sum_{i=1}^{N_F} \mathcal{S}(\boldsymbol{\rho}_i)}{N_F} - \mathcal{S}(\boldsymbol{\rho}) \right] + \left[ \left( \mathcal{S}(\boldsymbol{\rho}) - \sum_{i=1}^{N_F} \mathcal{S}(\boldsymbol{\rho}_i) \right) \times \sqrt{N_F} \right] \quad (5)$$

200 Where  $N_F$  is the number of factors (or communities) estimated by the Walktrap  
 201 algorithm,  $\mathcal{S}(\boldsymbol{\rho}_i)$  is the Von Neumann entropy for each individual factor and  $\mathcal{S}(\boldsymbol{\rho})$  is the  
 202 total entropy of the system of variables. Golino, Moulder, et al. (2020) showed that the Von  
 203 Neumann entropy can be approximately estimated in a correlation matrix by scaling it so  
 204 that the trace of the matrix equals one (i.e. taking a correlation matrix and dividing all  
 205 entries by the number of columns of the matrix). After scaling the correlation matrix, an  
 206 entropy-like metric can be obtained by the negative of the trace of the product of the density  
 207 matrix by the log of elements of the density matrix (see: Golino, Moulder, et al., 2020).

208 The TEFI index has two parts that can be separated as  $TEFI = [A] + [B]$  (Golino,  
 209 Moulder, et al., 2020). Element  $[A]$  is similar to that of the total correlation of multiple  
 210 variables (Watanabe, 1960), but instead of using the joint entropy for the partitions (factors  
 211 or clusters), it uses the total entropy of the system (i.e. entropy calculated using all variables  
 212 together). Additionally, the sum of the individual entropies (estimated per factor or cluster)  
 213 is divided by the number of partitions (i.e. factors or clusters), yielding what Watanabe  
 214 (2001) termed “K-function”. Element  $[B]$  reduces the influence of  $[A]$  by the number of  
 215 factors used to describe a given data set. As Golino, Moulder, et al. (2020) note, while  $[A]$  is  
 216 expected to decrease monotonically as the number of factors increases,  $[B]$  is expected to

217 increase as the number of factors increase.  $[B]$  represents the reduction in average entropy of  
218 a set of data conditional on a given factor or community structure. The square root of the  
219 number of factors was chosen in  $[B]$  in order to control the expected growth trajectory of  $[B]$   
220 as the number of factors increases. Golino, Moulder, et al. (2020) argues that the expected  
221 decrease in total entropy going from 1 to 2 factors would be higher than the expected  
222 decrease in entropy going from 100 to 101 factors, and therefore the multiplication by the  
223 square root of the number of factors is used to model this behavior.

## 224 Methods

225 In order to better understand the impact of varying the number of steps taken by the  
226 random walks,  $t$  will be adjusted from 3 to 10 within multiple data structures and  
227 community structure accuracy will be compared. The next paragraphs will describe the data  
228 generation mechanism used (a two-step approach), the design of the Monte Carlo simulation  
229 implemented and how the results are analyzed.

230 Data will be generated using a Monte Carlo simulation manipulating various data  
231 properties. First, a four factor structure and resulting correlation matrix will be estimated  
232 varying the sample size, continuous or categorical variables (4 categories), the number of  
233 variables per factor, whether or not the factors have the same number of variables within  
234 them, factor loadings, and the correlation between factors. When the number of variables  
235 within a community are unequal, two factors are reduced by one variable and two factors are  
236 increased by one variable (i.e., 8 variable factors have four factors containing 7, 7, 9, and 9  
237 variables). Relationships between the resulting variables will be estimated using either  
238 Pearson correlation, polychoric correlations (for categorical variables), or Louis-Guttman  
239 Image Structural Analysis (described below) and placed in a matrix.

240 **Data Generation**

241 The data generation mechanism used in the current paper follows a two-step approach.  
 242 The first step follows the common factor model used by Golino, Shi, et al. (2020), that works  
 243 as follows. First, the reproduced population correlation matrix (with communalities in the  
 244 diagonal) is computed:

$$\mathbf{R}_R = \mathbf{\Lambda}\mathbf{\Phi}\mathbf{\Lambda}', \quad (6)$$

245 where  $\mathbf{R}_R$  is the reproduced population correlation matrix, *lambda* ( $\mathbf{\Lambda}$ ) is a  $k \times r$  factor  
 246 loading matrix for  $k$  variables and  $r$  factors, and *phi* ( $\mathbf{\Phi}$ ) is the structure matrix of the latent  
 247 variables (i.e., a  $r \times r$  matrix of correlations among factors). This procedure implies that the  
 248 generated data does not contain correlated residuals (minor factors) at the population level.

249 The population correlation matrix  $\mathbf{R}_P$  is then obtained by inserting unities in the  
 250 diagonal of  $\mathbf{R}_R$ , thereby raising the matrix to full rank. Next, a Cholesky decomposition of  
 251  $\mathbf{R}_P$  is performed, such that:

$$\mathbf{R}_P = \mathbf{U}'\mathbf{U}. \quad (7)$$

252 If either  $\mathbf{R}_P$  is not semi-positive definite (i.e., at least one eigenvalue is  $\leq 0$ ) or an  
 253 item's communality is greater than 0.90, the  $\mathbf{\Lambda}$  matrix is replaced and a new  $\mathbf{R}_P$  matrix is  
 254 computed following the same procedure. Subsequently, the sample data matrix of continuous  
 255 variables is computed as:

$$\mathbf{X} = \mathbf{Z}\mathbf{U}, \quad (8)$$

256 where  $\mathbf{Z}$  is a matrix of random standard normal deviates with rows equal to the sample  
257 size and columns equal to the number of variables.

258 Following Golino, Shi, et al. (2020) cross-loadings with magnitudes consistent to those  
259 commonly found in real data (Bollmann, Heene, Küchenhoff, & Bühner, 2015) are randomly  
260 drawn from a normal distribution (with mean zero and variance of .15) for all the items  
261 except for the first two in each factor, which were set as markers (i.e., all of their  
262 cross-loadings are fixed to zero). Of note, regarding the generation of the main loadings: The  
263 function generates the main loadings by drawing random values from a uniform distribution  
264 that has a range of  $\pm .10$  from the specified value (so if the main loadings are set at 0.70, the  
265 function generates loading values between 0.60 and 0.80). The generated data is then used to  
266 compute an empirical correlation matrix  $\mathbf{C}_{\mathbf{X}}$ .

267 After estimating the data following the procedure described above, a second step is  
268 implemented. As indicated by Figure 1, the resulting correlation matrix of the simulated  
269 data (from the factor model;  $\mathbf{X}$ ) is then be multiplied by a predetermined undirected and  
270 unweighted network structure  $\mathbf{N}$  (with number and composition of communities equal to the  
271 number and composition of factors as simulated in the first step above) where the probability  
272 of nodes being linked within a community and between communities will be varied from low  
273 to high. The networks are simulated following the framework of Girvan and Newman (2002)  
274 for generating networks with specific (i.e., known) community structures. Multiplying  $\mathbf{C}_{\mathbf{X}}$  by  
275  $\mathbf{N}$  generates a matrix of weights  $\mathbf{W}$  with two important characteristics: the underlying  
276 factor structure is known (used to generate  $\mathbf{C}_{\mathbf{X}}$ ) and matches exactly the community  
277 structure of  $\mathbf{N}$ . The final sample data matrix of continuous variables is computed following a  
278 multivariate normal distribution with mean zero and variance-covariance matrix  $\mathbf{W}$ . The final  
279 sample data matrix contain continuous variables that can be discretized to generate  
280 polytomous data following the procedure described by Golino, Shi, et al. (2020).

281 This second step is necessary to control an important characteristic of networks that is

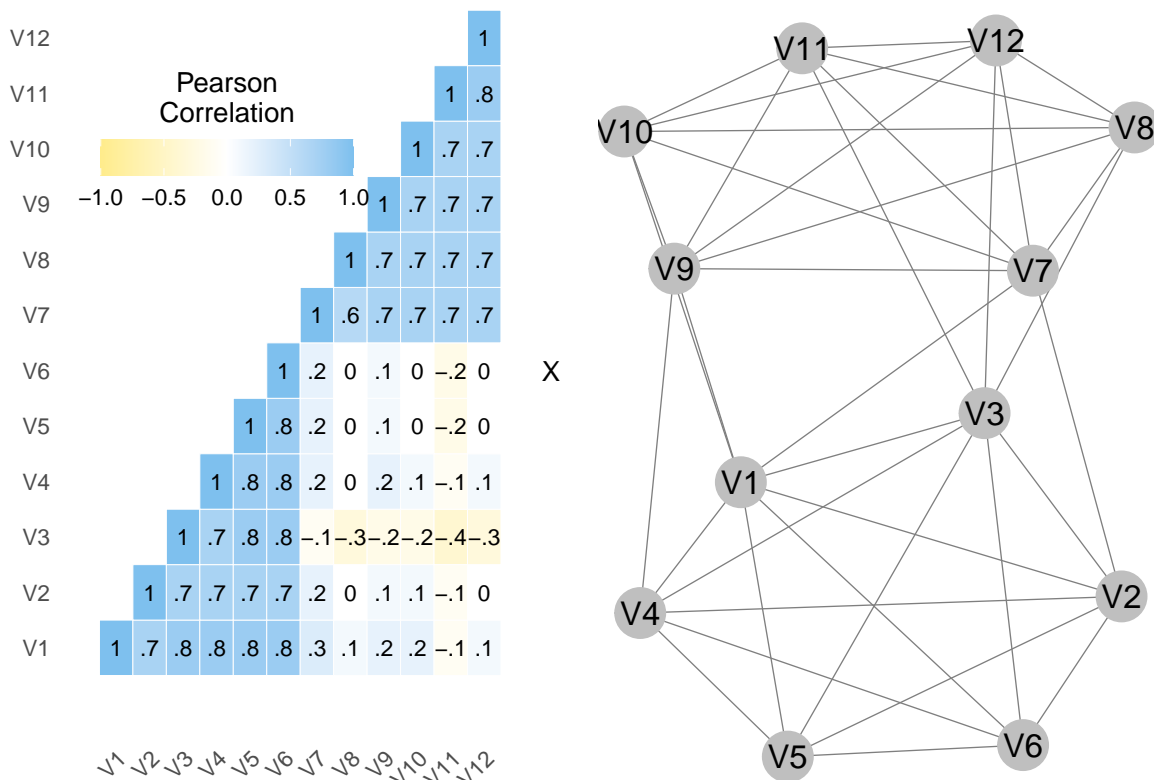


Figure 1. Network Data Generation

usually not controlled in the simulation studies employing the exploratory graph analysis  
 technique (e.g., Golino, Shi, et al., 2020): the link probabilities. Using a two-step data  
 generation approach is necessary to make the resulting data closer to real datasets.

In sum, data was generated in two steps: first, data is generated using a factor model  
 and the sample correlation matrix is obtained. In the second step a unweighted, undirected  
 network is generated and both matrices are multiplied to add a structural bias to the sample  
 correlation matrix obtained in the first step. This second portion can be thought of as adding  
 in spurious relationships at both the intra- and inter-community levels. We simulated a  
 network with a known number of communities (matching the data-generation mechanism of  
 the factor model), but with different levels of probabilities within and between communities  
 in terms of edges. Therefore, even if the true factor model has low interfactor correlations,  
 the structural bias will forcibly add edges between communities, or if the true factor model  
 has low factor loadings, the structural bias will forcibly add edges within communities. Due

295 to this methodology, we use the terms **factor** and **community** interchangeably.

296 All R code used in the current project are available in the Open Science Framework, as  
 297 well as the R Markdown manuscript integrating code and text for data analysis.

## 298 Design

299 To investigate the suitability of our algorithm to optimize the number of steps of the  
 300 Walktrap procedure, a Monte Carlo simulation was implemented and nine between-subject  
 301 data factors were systematically manipulated. Within the factor structure, the sample size  
 302 (500 and 1000), the equivalence in the number of variables per factor (i.e., whether or not all  
 303 factors have the same number of variables), number of variables per factor (4, 8), factor  
 304 loadings (.40 and .70), factor correlations (.30, .50 and .70), and type of variable (continuous  
 305 or polytomous with four response categories). Within the network structure, the probability  
 306 of links between communities (p-Out: .50 and .90), probability of links within communities  
 307 (p-In: .50, .75), and network method (glasso and TMFG) were manipulated. The  
 308 relationship between simulated variables was estimated either using traditional correlation  
 309 coefficients (Pearson for the continuous data condition and polychoric for the polytomous  
 310 data) or using the scaled covariance (or correlation) of images from Guttman’s Image  
 311 Structural Analysis (Guttman, 1953). In Guttman’s image structural analysis, the  
 312 covariance matrix of the *anti-images* ( $\mathbf{\Gamma}$ ) for  $n$  variables is:

$$\mathbf{\Gamma} = \mathbf{S}^2 \times \mathbf{R}^{-1} \times \mathbf{S}^2$$

313 where  $\mathbf{S}^2$  is the diagonal matrix with the anti-norms ( $\mathbf{S}^2 = \text{Diag} \left( \frac{\Delta(\mathbf{R})}{\Delta(R_{ii})} \right)$ ), being  $\Delta\mathbf{R}$  the  
 314 determinant of  $\mathbf{R}$  and  $\Delta(R_{ii})$  the cofactor of  $R_{ii}$ ), and  $\mathbf{R}^{-1}$  is the inverse of the correlation  
 315 matrix  $\mathbf{R}$ . The covariance matrix of the *images* ( $\mathbf{G}$ ) is:

$$\mathbf{G} = \mathbf{R} + \mathbf{\Gamma} - 2\mathbf{S}^2$$

316 Guttman (1953) proposed a theorem in which any correlation coefficient can be  
 317 regarded as the difference between two covariances, one for the common parts between the  
 318 variables (images) and another by the alien parts (anti-images). This theorem leads to an  
 319 important paradox, that the alien parts (i.e., the covariance of the partial anti-images) are  
 320 more important to the structural analysis of a correlation matrix than the common parts  
 321 (i.e., the covariance of the partial images), because a correlation matrix can be computed  
 322 using only the partial anti-norms and the covariance of the anti-images (i.e.,  
 323  $\mathbf{R} = \mathbf{S}^2 \times \mathbf{\Gamma}^{-1} \times \mathbf{S}^2$ ), but cannot be computed using the covariance of the images.  
 324 Commonness in image structural analysis comes from the use of a multiple-regression  
 325 approach in which correlations can be explained by means of the multiple regression of each  
 326 variable on the remaining  $n-1$  variables. Guttman’s image structural analysis was linked to  
 327 factor analysis in several classical works (Harman, 1976; Harris, 1962), and here the scaled  
 328 covariance matrix of the images is also used, to be contrasted to the results obtained using  
 329 traditional (Pearson or polychoric) correlation estimation techniques. The goal in using  
 330 Guttman’s image structural analysis is to investigate its effect in the accuracy of the  
 331 Walktrap algorithm used in the EGA framework.

332 This design results in 1536 conditions to be compared. For each condition, 500  
 333 datasets were simulated.

## 334 Data Analysis

335 **Assessing Accuracy of Cluster Partitions.** For each simulated dataset,  $TEFI$   
 336 values from  $t = 3$  to  $t = 10$  will be compared. The model with the lowest value of  $TEFI$  will  
 337 be identified and the structure and accuracy of the partition will be compared to  $t = 4$  as



338 seen in Figure 2.

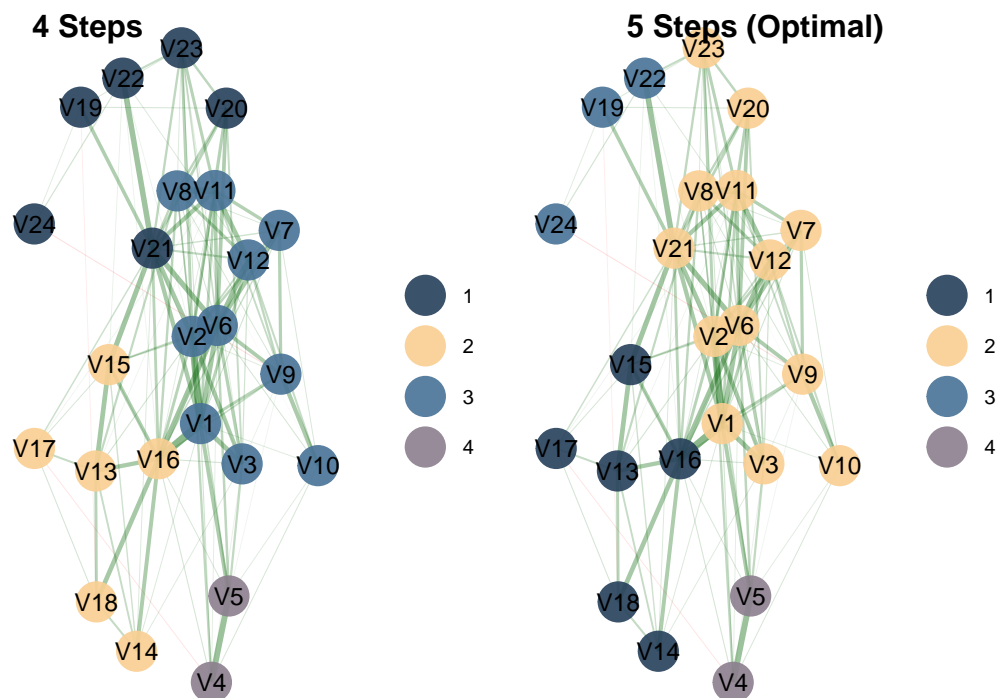


Figure 2. Default vs. Optimal Estimated Structure

339 The accuracy of a partition is considered to be higher when nodes sharing high edge  
 340 weights are assigned to the same cluster while nodes sharing comparatively lower edge  
 341 weights are assigned to separate clusters. The current paper will employ multiple measures  
 342 of fit to assess the accuracy of the Walktraph algorithm: Majority Placement (MP), the  
 343 Hubert-Arabie Adjusted Rand Index ( $ARI_{HA}$ ), and Normalized Mutual Information (NMI).  
 344 Additionally we use an overall measure of accuracy coded as 1 when the correct number of  
 345 communities was discovered and 0 otherwise.

346 **Majority Placement.** Majority placement (MP) is a classification rate assessing  
 347 the portion of nodes correctly classified (Gates et al., 2016; Girvan & Newman, 2002) If a  
 348 node is placed in a community with more than 50% (the majority) of all other nodes from its  
 349 true community then it is defined as being in its true community (Fortunato, 2010). More  
 350 formally,

$$MP = \sum_{i=1}^N \frac{\tau_i}{N}, \left\{ \begin{array}{l} 1 \text{ if node } i \text{ is placed with } \geq 50\% \text{ of nodes from its true community} \\ 0 \text{ otherwise} \end{array} \right. \quad (9)$$

351 where for each node  $i$ ,  $\tau_i$  is 1 if the node is in a community with 50% or more of other  
 352 nodes from its true community. Note that this metric becomes unreliable if there are fewer  
 353 communities identified than in the true structure (e.g., if only one community is detected, all  
 354 nodes are placed with  $\geq 50\%$  of the nodes from their true community).

355 **Hubert-Arabie Adjusted Rand Index.** Given the potential biases of relying  
 356 solely on MP, we are additionally employing the *Hubert-Arabie Adjusted Rand Index* ( $ARI_{HA}$ ;  
 357 (Hubert & Arabie, 1985)).  $ARI_{HA}$  provides complementary information to the MP however it  
 358 has more rigid constraints on what constitutes correct placement (Gates et al., 2016;  
 359 Steinley, 2004). There are penalizations for pairing nodes in the same community if they are  
 360 not paired in the true structure, and vice versa. In this way,  $ARI_{HA}$  penalizes the quality of  
 361 fit for identifying fewer communities than exist in the true structure.

362  $ARI_{HA}$  is formally defined as:

$$ARI_{HA} = \frac{\binom{N}{2}(a+d) - [(a+b)(a+c) + (c+d)(b+d)]}{\binom{N}{2} - [(a+b)(a+c) + (c+d)(b+d)]} \quad (10)$$

363 where  $a$  represents the number of paired nodes, in the same community, both in the  
 364 true and recovered cluster solution;  $b$  represents the number of nodes paired in the same  
 365 community in the true structure that were not paired in the same community in the  
 366 recovered structure;  $c$  represents the number of nodes not paired in the same community in  
 367 the true structure that were paired in the same community in the covered structure; and  
 368 finally,  $d$  represents the number of node pairs that are not in the same community in both

369 the true and recovered structure.  $\text{ARI}_{\text{HA}}$  was implemented using the clues package in R  
 370 (Chang et al., 2010).

371 **Normalized Mutual Information.** Normalized mutual information (NMI)  
 372 compares the true and recovered partitions by creating a confusion matrix where rows  
 373 represent true communities and columns represent recovered communities (Danon,  
 374 Diaz-Guilera, Duch, & Arenas, 2005).  $N_{ij}$  is the node in true community  $i$  that also appears  
 375 in the recovered community  $j$ . This matrix is then used to assess the similarity of partitions.  
 376 Formally, NMI is defined as:

$$I(A, B) = \frac{-2 \sum_{i=1}^{c_A} \sum_{j=1}^{c_B} N_{ij} \log\left(\frac{N_{ij}}{N_{i.} N_{.j}}\right)}{\sum_{i=1}^{c_A} N_{i.} \log\left(\frac{N_{i.}}{N}\right) + \sum_{j=1}^{c_B} N_{.j} \log\left(\frac{N_{.j}}{N}\right)} \quad (11)$$

377 where  $N_{ij}$  represents a matrix in which  $A$  represents a vector of true communities,  $B$   
 378 represents a vector of recovered communities,  $c_A$  and  $c_B$  denote the number of communities  
 379 in either  $A$  or  $B$ , the sum of row  $i$  is denoted by  $N_{i.}$ , and the sum of column  $j$  is denoted by  
 380  $N_{.j}$ . NMI has a maximum of 1, the true and recovered communities are identical, and a  
 381 minimum of 0, when no true communities are recovered.

382

## Results

383 Comparing  $TEFI$  across all values of  $t$ , the lowest  $TEFI$  value within 49.7% of the  
 384 simulated datasets were obtained by a value other than  $t = 4$ . Within all values of  $t$  other  
 385 than 4, Figure 3 represents the proportion of datasets where each value of  $t$  provided the  
 386 optimal fit (i.e., the lowest  $TEFI$  value).

387 The question then becomes how does the optimal dimensionality structure (i.e., the  
 388 structure with the lowest  $TEFI$ ) compare to the default structure (i.e., the structure  
 389 estimated with  $t = 4$ ) when the optimal model is selected for a value of  $t$  other than 4. To

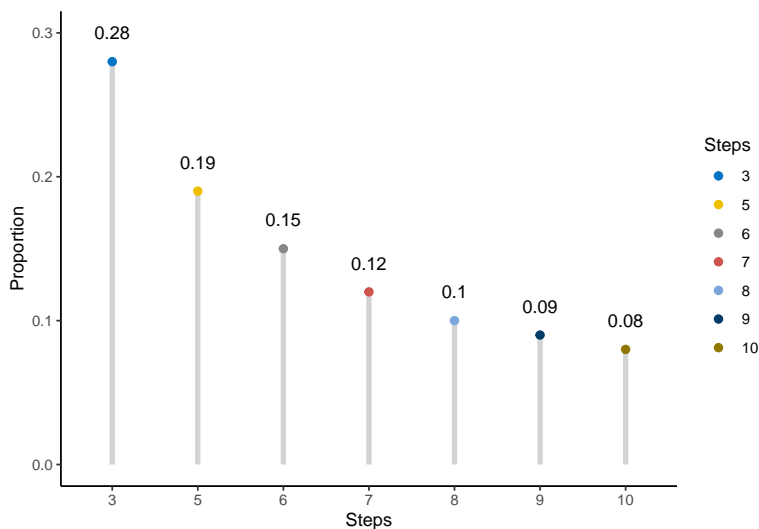


Figure 3. Proportion of Optimal Steps Within  $t$  Other Than 4

390 investigate this, we evaluated the interaction between each data factor. A 10-way ANOVA  
 391 across all data factors was conducted using change in overall accuracy, MP, ARIHA, and  
 392 NMI. Change in a given metric was computed by the metric value at the optimal number of  
 393 steps minus the metric value at  $t = 4$  for those datasets where the default structure  
 394 estimated was not the structure estimated using the optimized number of steps. We recorded  
 395 the effect size of each main effect and interaction using partial eta squared ( $\eta_p^2$ ) following the  
 396 guidelines of Cohen (2013) where values of 0.01 represent small effects, 0.06 medium effects,  
 397 and 0.14 or more large effects.

398 For each metric, a greater positive difference between the optimal structure and the  
 399 default structure is preferred. For instance, if the optimal structure for a given dataset had a  
 400 MP value of 0.5 and the default structure had a MP value of 0.1, then the difference in MP  
 401 would be  $0.5 - 0.1 = 0.4$ , indicating a gain in majority placement when the number of steps  
 402 is optimized using the TEFI index. However, if the optimal structure had a MP value of 0.4  
 403 and the default structure had a MP value of 0.5, then the difference in MP would be  
 404  $0.4 - 0.5 = -0.1$ , indicating that by optimizing the number of steps the resulting structure  
 405 has a lower majority placement value.

406 There were several data structures that exhibited no main effect or interaction after  
 407 evaluating  $\eta_p^2$ . However, two such data conditions exhibited interesting results when visually  
 408 inspecting change in accuracy metrics. 4 shows differences in the interaction between  
 409 network estimation method and correlation type when split by variable type. When using  
 410 Louis-Guttman Image Structural Analysis, we see slight improvement in accuracy for  
 411 polytomous data regardless of network estimation method and improvement in MP when  
 412 using *glasso*.

413 Additionally, we found small differences (as seen in Figure 5), a result that's in the  
 414 opposite direction of what is obtained in the same conditions but for the traditional  
 415 correlation techniques. For this data condition, we see improvements both in majority  
 416 placement and accuracy.

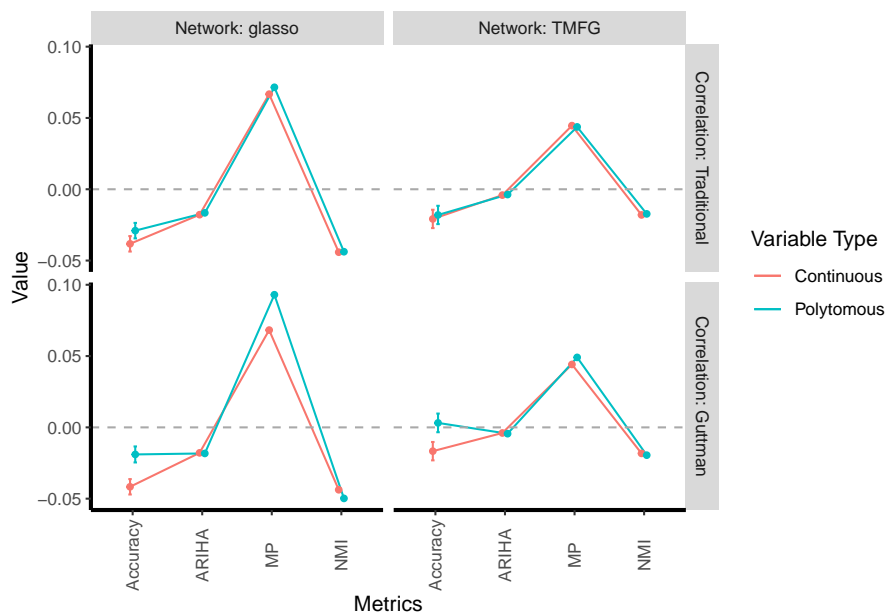


Figure 4. Interaction between Network Estimation and Correlation Type by Variable Type

417 Figure 6 shows the overall interaction of interfactor correlations, factor loadings, the  
 418 probability of node connections within communities, and the probability of node connections  
 419 between communities split by the number of variables per community and the type of  
 420 variable. In general, four variables per community do not see marked improvement in any

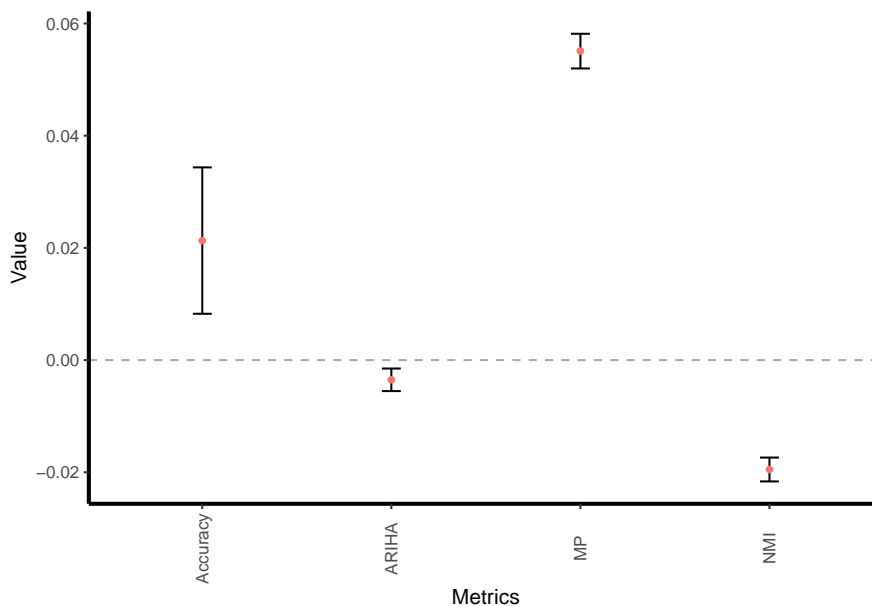


Figure 5. Effect with Sample Size of 1000, Using Louis-Guttman Image Structural Analysis, Number of Variables Is Not Equal Across Factors, TMFG Network Estimation, and Polytomous Variables

421 metric except for MP. Eight variables per community, however, is in general associated with  
 422 greater improvement across each metric. This relationship is most notable and consistent  
 423 within accuracy. When p-Out is lower, 0.5, number of variables per community is 8, as  
 424 interfactor correlations increase so does the improvement in accuracy, regardless of factor  
 425 loadings. However, when p-Out is higher, 0.9, the opposite is true. For 8 variables per  
 426 community, as interfactor correlations increase, there is a decrease in the improvement of  
 427 accuracy. In both scenarios the change in other metrics remain constant with the exception  
 428 of MP. When p-Out = 0.90, there is a slight upward trend in the improvement of MP as  
 429 interfactor correlations increase for both 4 and 8 variable per factor.

430 The relationship between interfactor correlations, factor loadings, and p-In and p-Out  
 431 remain constant regardless of variable type. Interestingly, the trend in accuracy improvement  
 432 as interfactor correlations increase seen when split by variable type for p-Out = 0.50 is no  
 433 longer notable when split by variable type. However, when p-Out = 0.90, the improvement  
 434 in accuracy still decreases as interfactor correlation increases and the improvement in MP

435 still increases as interfactor correlation increases.

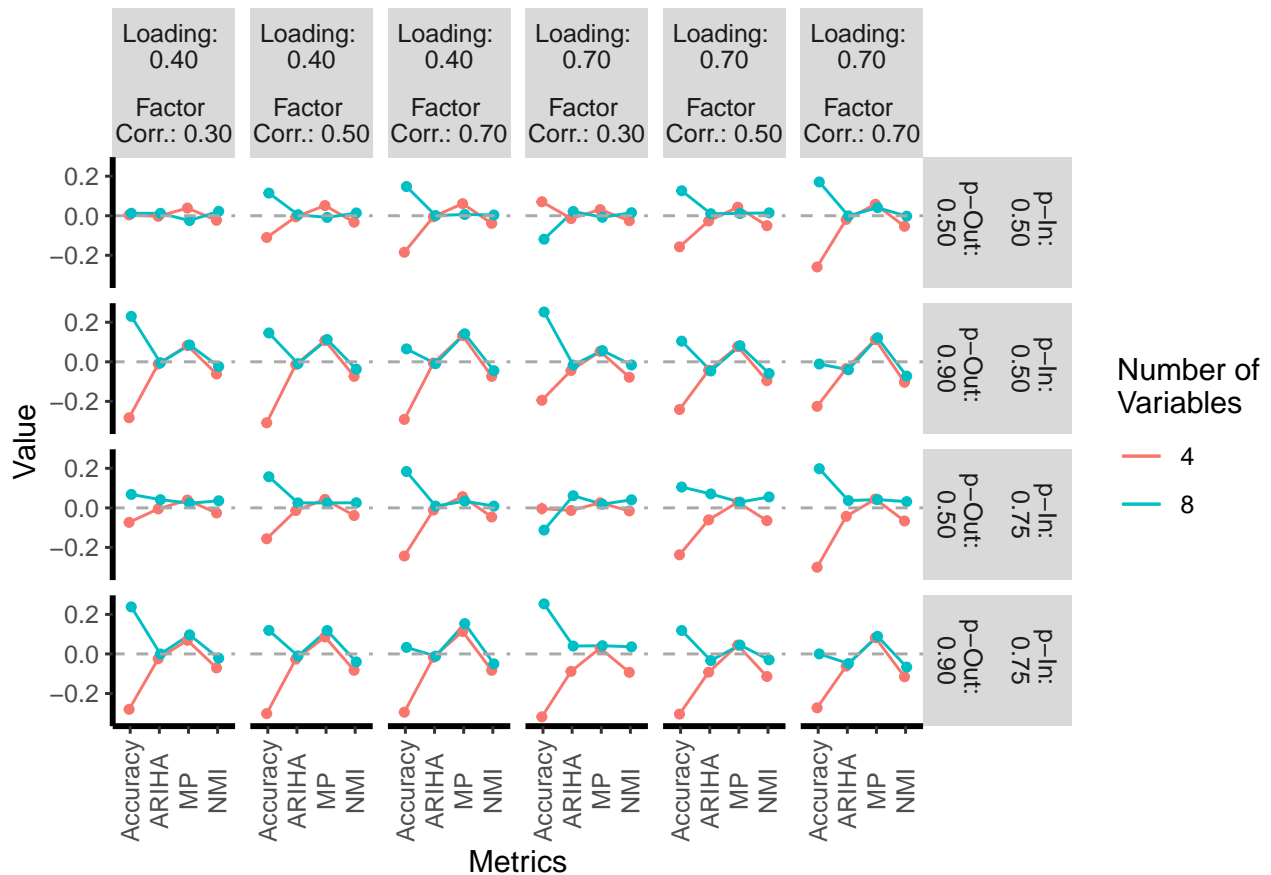


Figure 6. Interaction between Factor Loadings (Loading), Factor Correlations (Factor Corr.), p-In and p-Out by Number of Variables

436 Since most, if not all, of psychological measurement relies on polytomous response  
 437 variable, and the larger effects of tuning the number of steps used in the Walktrap algorithm  
 438 were seen in polytomous data conditions with more variables per factor (i.e., 8), the  
 439 remainder of results will be reported on these conditions only and one 8-way ANOVA was  
 440 conducted for these data structures. Table 1 shows the effect sizes for each effect from this  
 441 model.

442 Figures 8, 9, and 10 show the 3 effects showing at least a small effect size ( $\eta_p^2 > 0.01$ ).  
 443 As seen in Figure 8, when p-In is greater (0.75), there is a slight improvement in each metric  
 444 change compared to p-In at 0.50. Similarly, Figure 9 when p-Out is greater (0.90) and  
 445 interfactor correlation is lower (0.30) there is greater improvement in accuracy and MP.

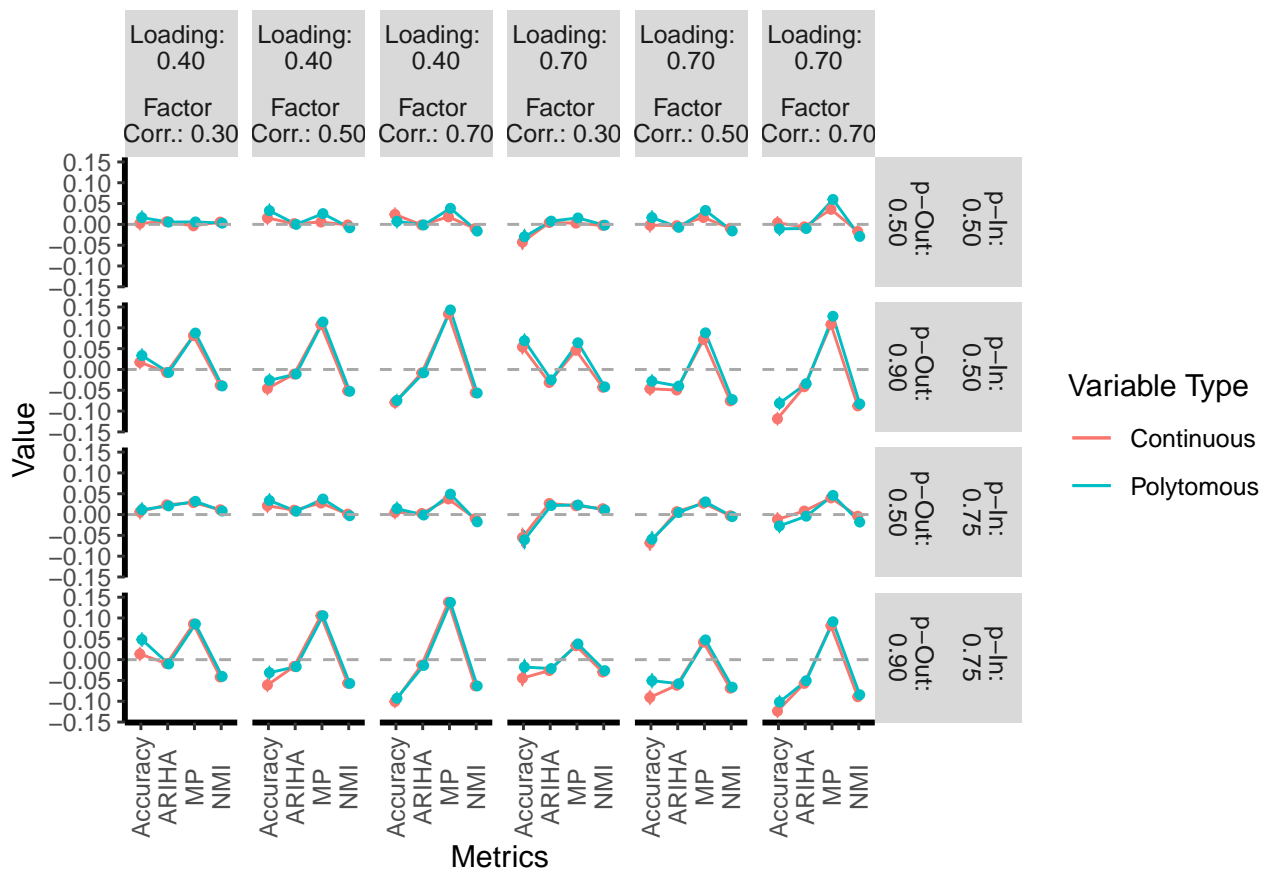


Figure 7. Interaction between Factor Loadings (Loading), Factor Correlations (Factor Corr.), p-In and p-Out by Variable Type

446 However, as interfactor correlation increases, this relationship is no longer consistent. Within  
 447 p-Out at 0.50, as interfactor correlations increase there is an increase in the gain for accuracy  
 448 but the other three metrics remain constant. Overall, the proposed method shows  
 449 improvement in both accuracy and MP across levels of interfactor correlation, and presents  
 450 the larger gains when there's more structural bias (i.e., larger interfactor correlations and  
 451 lower p-Out, and lower interfactor correlations and high p-Out).

452 Finally, 10 is split by factor loadings where we see a similar relationship within p-Out  
 453 at 0.90 where this is a more notable increase in accuracy and MP. When p-Out is lower (0.50)  
 454 as factor loadings increase, there is a slight gain in each metric. Interestingly, across all three  
 455 plots in Figures 8, 9, and 10 we see little to no improvement in NMI and  $ARI_{HA}$  and a  
 456 majority of the improvement is notable in Accuracy and MP. Again, as happened with the



Table 1

*Effect Size by Effect Tested for 8 Polytomous Variables per Factor*

	Accuracy	ARIHA	MP	NMI
Network	0.000	0.001	<b>0.011</b>	0.006
CORF	0.001	<b>0.014</b>	<b>0.015</b>	<b>0.029</b>
P.OUT	0.000	<b>0.041</b>	<b>0.064</b>	<b>0.100</b>
CORF:P.OUT	<b>0.017</b>	0.002	0.001	0.005

457 p-Out link probability and interfactor correlation pairing, the larger the structural bias, the  
 458 bigger the gain in accuracy and majority placement for the p-In and factor loadings pairing.

459

### Empirical Example

460 To demonstrate the use of our approach to tune the number of steps used in the  
 461 Walktrap algorithm used in exploratory graph analysis, we apply this method to the  
 462 Developmental Coordination Disorder Questionnaire (DCDQ: Schoemaker et al., 2006). Data  
 463 was provided to us through the Simons Foundation Powering Autism Research for Knowledge  
 464 (SPARK) of the Simons Foundation Autism Research Initiative (SFARI), a large research  
 465 initiative which has collected data from over 50,000 individuals with autism and their  
 466 families (Feliciano et al., 2018). The DCDQ is a questionnaire given to parents of children  
 467 (aged 5 to 15) to assess Developmental Coordination Disorder (DCD) commonly seen in  
 468 individuals with autism spectrum disorders. DCD manifests as subtle motor skill impairment  
 469 which affect things such as handwriting, clumsiness, energy levels, and athletic ability.

470 A grid search was conducted across values of  $t$  using EGA. Relationships between  
 471 variables were estimated using partial correlation and the network was estimated using  
 472 glasso. Figure 11 shows the  $TEFI$  values across each level of  $t$ . When using the default  
 473  $t = 4$ ,  $TEFI = -7.64$ . The lowest value of  $TEFI$  (-9.72) occurs when  $t = 9$ . These results  
 474 indicate that  $t = 9$  provides the optimal model for this dataset. Figure 12 shows the  
 475 difference in estimated community structure across  $t = 4$  and  $t = 9$ .

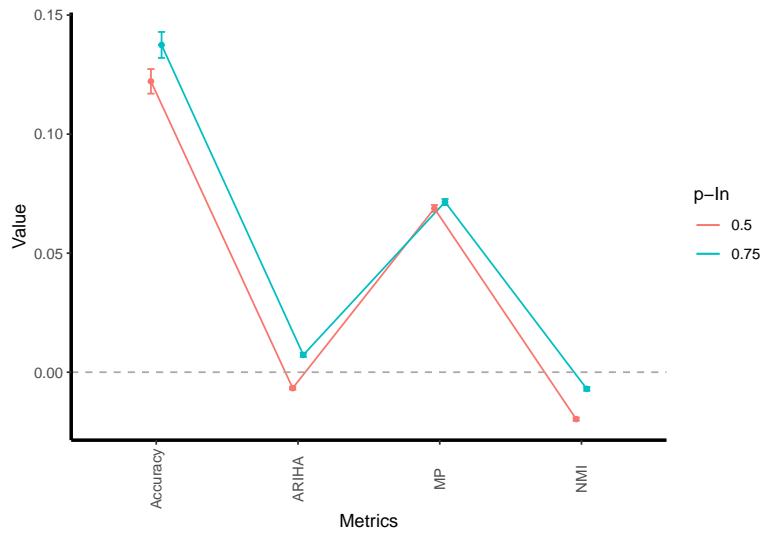


Figure 8. p-In Effect for 8 Polytomous Variables per Factor

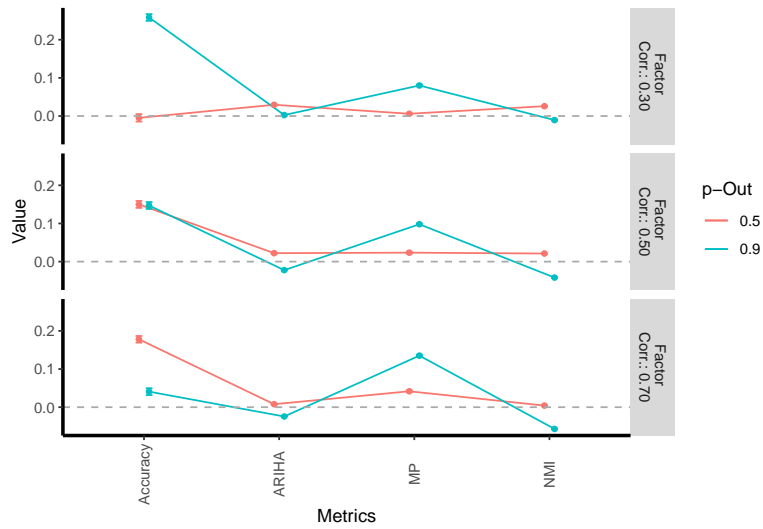


Figure 9. Interaction between p-Out and Factor Correlations (Factor Corr.) for 8 Polytomous Variables per Factor

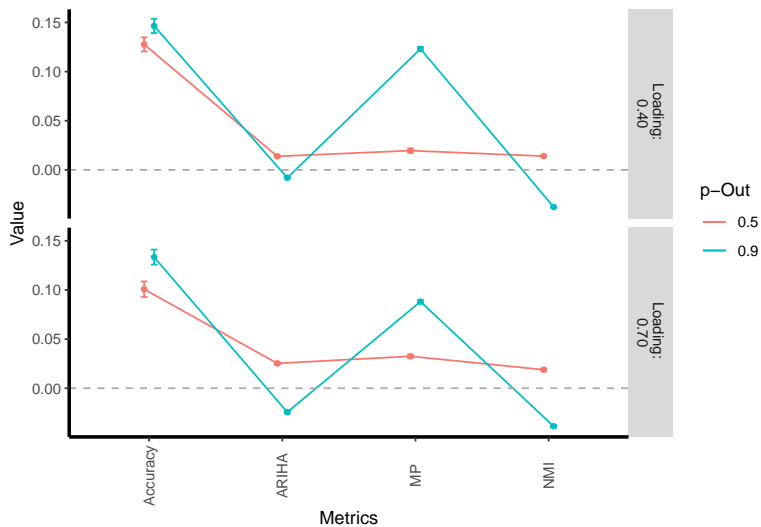


Figure 10. Interaction between p-Out and Factor Loadings (Loading) for 8 Polytomous Variables per Factor

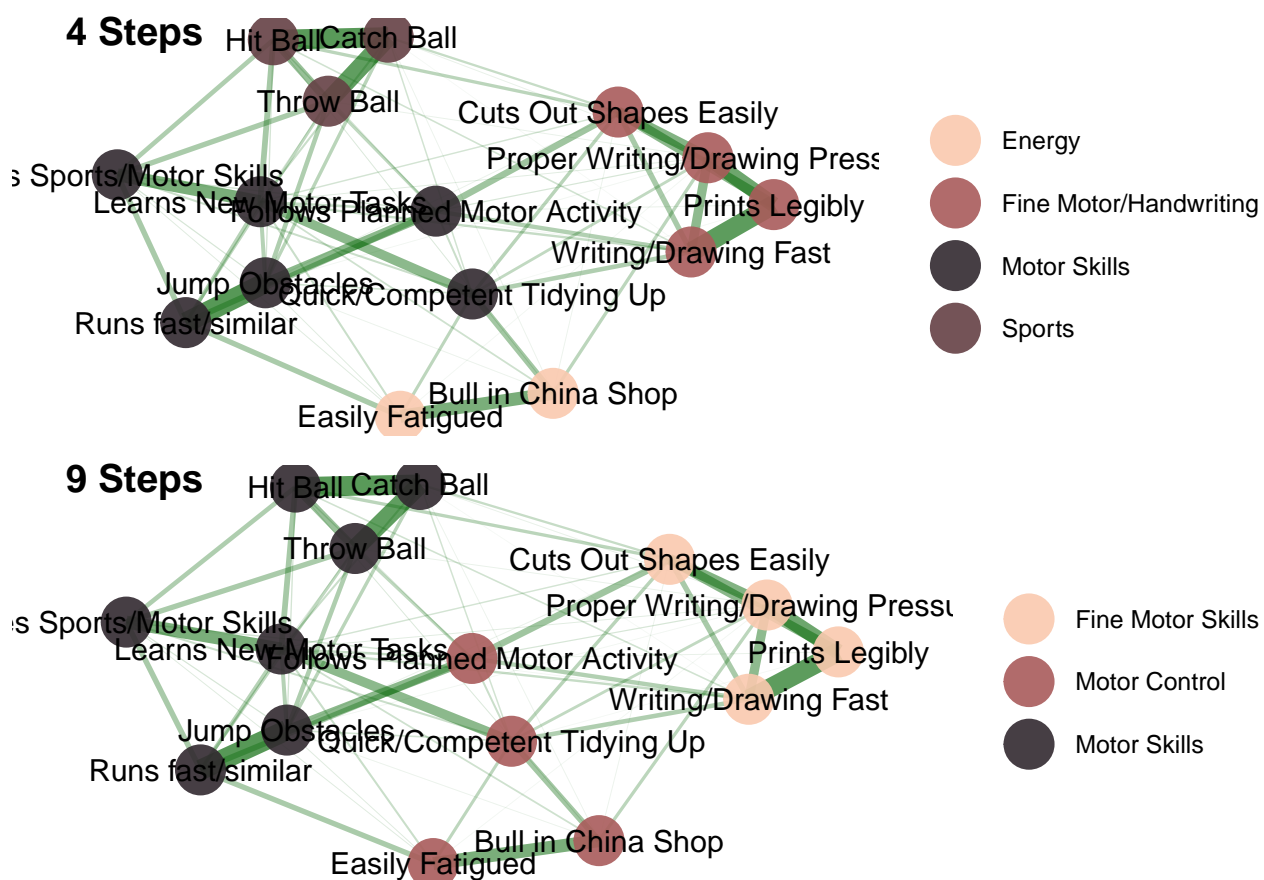


Figure 12. DCDQ Graph Estimations

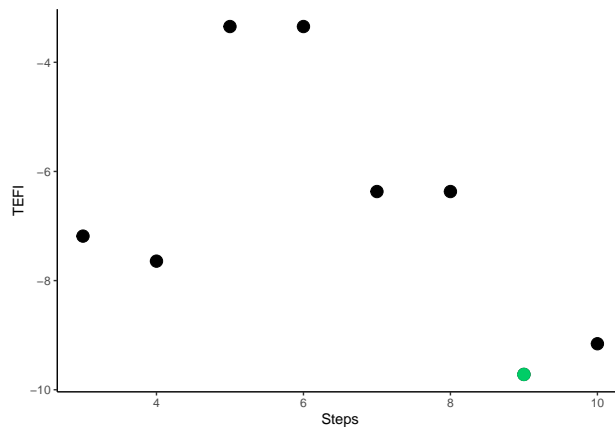


Figure 11. DCDQ TEFI Across Values of  $t$

476 Table 2 shows the items of the DCDQ along with which scales they loaded onto from  
 477 the original scale validation compared to the dimensions identified by EGA with an  
 478 optimized  $t$  value. The *TEFI* value obtained by the optimal EGA model (-9.72) is lower  
 479 than the *TEFI* value obtained by the original factor structure (-9.25). Both analyses  
 480 revealed three very similar dimensions. However, the dimensionality uncovered by EGA  
 481 using the proposed method moved items into slightly different positions within the  
 482 community structure which in turn adjusts the interpretation of these communities.

Table 2  
*Comparing DCDQ Dimensionality Assessments*

Item	Original Factor Analysis: TEFI = -9.25	Optimal EGA: TEFI = -9.72
Throws ball in a controlled and accurate fashion.	1. Control During Movement	1. Motor Skills
Catches a small ball from a distance.	1. Control During Movement	1. Motor Skills
Hits an approaching ball or birdie with a bat or racquet accurately.	1. Control During Movement	1. Motor Skills
Jumps easily over obstacles found in garden or play environment.	1. Control During Movement	1. Motor Skills
Runs as fast and in a similar way to other children of the same gender and age.	1. Control During Movement	1. Motor Skills
Is interested in and likes participating in sports or active games requiring good motor skills.	3. General Coordination	1. Motor Skills
Learns new motor tasks easily and does not require more practice or time than other children to achieve the same level of skill.	3. General Coordination	1. Motor Skills

Table 2  
*Comparing DCDQ Dimensionality Assessments (continued)*

Item	Original Factor Analysis: TEFI = -9.25	Optimal EGA: TEFI = -9.72
Cuts out pictures and shapes accurately and easily.	2. Fine Motor/Handwriting	2. Fine Motor Skills
Printing, writing, or drawing is fast enough to keep up with the rest of the children.	2. Fine Motor/Handwriting	2. Fine Motor Skills
Printing or writing of letters, numbers, and words is legible, precise, or accurate.	2. Fine Motor/Handwriting	2. Fine Motor Skills
Uses appropriate effort or tension when printing, writing, or drawing.	2. Fine Motor/Handwriting	2. Fine Motor Skills
Can follow their plan of motor activity and organize their body to effectively complete the task.	1. Control During Movement	3. Motor Control
Child is quick and competent in tidying up, putting on shoes, dressing, etc.	3. General Coordination	3. Motor Control
Could be described as a 'bull in a china shop' (appears clumsy, might break fragile things in a small room)	3. General Coordination	3. Motor Control

Table 2  
*Comparing DCDQ Dimensionality Assessments (continued)*

Item	Original Factor Analysis: TEFI = -9.25	Optimal EGA: TEFI = -9.72
Fatiues easily, appears to slouch and 'fall out' of the chair if required to sit for long periods.	3. General Coordination	3. Motor Control

483 All items related to fine motor skills and writing were identified in both analyses as a  
484 complete factor. Items related to sports and the enjoyment/proficiency of motor skills were  
485 assigned to the same community by EGA. In the original factor structure, whether or not  
486 the child enjoyed sports or enjoyed learning new motor skills did not load on to the same  
487 factor as items related to their abilities (e.g., throwing, catching, or hitting a ball). The item  
488 relating to whether or not the child is interested in participating in sports loaded onto a  
489 factor labeled “general coordination” with other items related to clumsiness, ability to clean  
490 up, and energy level. From a face valid standpoint, while these items are related generally to  
491 motor skills and coordination, it does not seem that they account for a similar type of  
492 variance in the overall construct. Rather the third community identified by EGA in this  
493 analysis appears to be more cohesive containing items related to ability to plan and  
494 accurately execute a task, ability to complete a task such as tidying up, and levels of  
495 clumsiness and fatigue.

## 496 Discussion

497 The Walktrap algorithm is a widely used community detection algorithm within  
498 network psychometrics particularly for estimating latent factors. However, the Walktrap  
499 algorithm contains a hyperparameter ( $t$ ) the properties of which have not been fully  
500 researched. The present study tested a grid search approach for tuning  $t$ , identifying the  
501 optimal model with *TEFI*. Using synthetic data following data structures commonly found  
502 in psychological research, the benefits in model accuracy using this approach were  
503 investigated.

504 Data was simulated by multiplying a matrix of variables following a common factor  
505 model by a unweighted, undirected network to add a structural bias to the sample  
506 correlation matrix. 500 datasets were simulated across 1536 varied data structures, similar to  
507 the wide variety of structures found in substantive psychometric research. EGA was



508 implemented varying the number of steps used by the Walktrap algorithm from 3 to 10. The  
509 optimal model with the lowest *TEFI* value was identified and compared to the model at  
510  $t = 4$ . Using overall accuracy, MP, ARIHA, and NMI as measures of partition accuracy, an  
511 analysis was conducted to identify whether or not and which kind of data structures benefit  
512 from varying  $t$ .

513 The results indicate that especially as sampling error is introduced into data, varying  
514 the number of steps within the Walktrap algorithm is beneficial. Importantly, it was  
515 demonstrated that the proposed method functioned similarly for both continuous and  
516 polytomous data. In line with previous dimensionality assessment research, the proposed  
517 method was particularly effective with a higher number of variables per factor (Garrido,  
518 Abad, & Ponsoda, 2011) as well as work in factor analysis positing that the increase in  
519 indicators also increases model error (MacCallum, Widaman, Preacher, & Hong, 2001).

520 As a higher probability of spurious intercommunity connections is introduced, the  
521 proposed method showed improvement over the traditional method both in estimating the  
522 correct number of communities but also the probability that nodes will be placed with other  
523 nodes from their true community. Spurious intercommunity connections not only interact  
524 with interfactor correlations, but also factor loadings. As the probability of spurious  
525 intercommunity connections increases, the proposed method provides improved model  
526 estimation. These findings are also in line with prior research indicating that higher  
527 interfactor correlations and lower loadings present particular challenges in accurate  
528 dimensionality assessment (Garrido et al., 2011; Garrido, Abad, & Ponsoda, 2013; Lubbe,  
529 2019). Finally, when using Louis-Guttman Image Structural analysis as opposed to  
530 traditional correlations, there was a greater improvement in MP for polytomous data. The  
531 greatest metric improvement provided by the proposed method was seen in Accuracy and  
532 MP. These both relate directly to important aspects of how dimensionality assessment  
533 influences substantive research.

534 When substantive researchers validate a new measure, dimensionality assessment is  
535 often one of the first steps taken. As scales are broken down into further subscales, the facets  
536 of the larger latent structure being measured become clearer. In terms of structural validity,  
537 researchers and clinicians rely on the theory that scores and their variation directly relate to  
538 the structure of the scale and its subscales (Borsboom, Mellenbergh, & Van Heerden, 2004;  
539 Steger, 2006). As such, it is vital that any method applied to assess the relationship among  
540 items and the dimensionality of a scale is optimized to estimate the correct number of  
541 dimensions as well as place items together that assess the same dimension.

542 Flores-Kanter, Garrido, Moretti, and Medrano (2021) provide a great example of this  
543 using the Positive and Negative Affective Scale (PANAS; Watson, Clark, & Tellegen, 1988)  
544 where they review the multitude of studies evaluating its structure and discuss the  
545 implication of inconsistent structures estimated using traditional factor analytic techniques.  
546 In its validation, the PANAS was first identified as a three factor model: Positive Affect,  
547 Afraid, and Upset. These two negative affect scales (Afraid and Upset) represent orthogonal  
548 structures that many studies lump together as unidimensional. Flores-Kanter et al. (2021)  
549 evaluate the PANAS with EGA to assess the dimensionality (and stability thereof) and  
550 reveal a structure almost identical to the original three factor model. Similarly, the empirical  
551 example outlined in the current paper demonstrates the differences in scale interpretation  
552 based on the estimated factor structure. For both scales, the application of advanced and  
553 optimized methodology provided a clearer and more interpretable structure than traditional  
554 methods.

555 For the current study, it should be noted that in the data generation method, we  
556 introduced structural bias to better imitate empirical datasets. Therefore, error is introduced  
557 into model results not just from the model estimation process, but also from simulated  
558 sampling error. As a result, the magnitude of  $\eta_p^2$  was impacted and no large effect sizes were  
559 found. Nonetheless, small and medium effect sizes revealed interesting relationships.

560 While the current paper reports rigorous testing of the proposed method in over 1500  
561 combinations of common data structures, there are still several conditions not manipulated.  
562 For example, the proposed method was only tested for a four factor structure and also did  
563 not investigate how the method performs in very large networks (e.g., over 100 nodes).  
564 Additionally, the data generation method did not incorporate population error as it is  
565 traditionally implemented in psychometric literatur (Montoya & Edwards, 2020).

566 Future expansion on the current research should investigate the same application with  
567 different fit indices beyond *TEFI* (e.g., AIC and BIC). While the current method has been  
568 shown to work well in cross-sectional factor designs, additional research should be conducted  
569 expanding into dynamical systems. Finally, particularly within polytomous data, additional  
570 work should be conducted investigating how this method functions when variables are  
571 skewed.

## 572 Conclusion

573 Proper latent trait modeling is the crux of almost every portion of psychological  
574 research. Many theories and statistical methods have been developed to assess the  
575 dimensionality of latent variables, each with its own strengths and weaknesses. EGA has  
576 been shown to perform well (and above and beyond similar methods) across data structures  
577 commonly found in psychological research. We aim to improve EGA even further by  
578 introducing a new technique when using the Walktrap algorithm for community detection.  
579 Instead of following standard guidelines statically setting  $t$ , a grid search can be conducted  
580 to optimize select the optimal value of  $t$ . In order to select the optimal value of  $t$ , we  
581 recommend using *TEFI* due to its advantages in detecting the correct dimensionality  
582 solution.

583 The proposed method was tested across a variety of data structures commonly found

584 in psychological research (e.g., highly correlated factors with spurious connections collected  
585 with polytomous response data). It was found to provide improvement above and beyond  
586 traditional methodology for the Walktrap algorithm in identifying the dimensionality and  
587 specific item-community organization. Additionally, the method was applied to a substantive  
588 dataset and shown to provide a clearer and more cohesive structure than both the original  
589 factor structure and the dimensionality structure identified by the traditional Walktrap  
590 application.

## References

591

592 Bollmann, S., Heene, M., Küchenhoff, H., & Bühner, M. (2015). *What can the real world do*  
593 *for simulation studies? A comparison of exploratory methods*. LMU. Retrieved from  
594 Department%20of%20Statistics,%20University%20of%20Munich:%20https:  
595 //epub.ub.uni-muenchen.de/24518/

596 Borsboom, D. (2017). A network theory of mental disorders. *World Psychiatry, 16*(1), 5–13.

597 Borsboom, D., Mellenbergh, G. J., & Van Heerden, J. (2004). The concept of validity.  
598 *Psychological Review, 111*(4), 1061.

599 Bringmann, L. F., Vissers, N., Wichers, M., Geschwind, N., Kuppens, P., Peeters, F., . . .  
600 Tuerlinckx, F. (2013). A network approach to psychopathology: New insights into  
601 clinical longitudinal data. *PloS One, 8*(4), e60188.

602 Chang, F., Qiu, W., Zamar, R. H., Lazarus, R., Wang, X., & others. (2010). Clues: An r  
603 package for nonparametric clustering based on local shrinking. *Journal of Statistical*  
604 *Software, 33*(4), 1–16.

605 Chen, J., & Chen, Z. (2012). Extended bic for small-n-large-p sparse glm. *Statistica Sinica,*  
606 555–574.

607 Christensen, A. P., Cotter, K. N., & Silvia, P. J. (2019a). Reopening openness to experience:  
608 A network analysis of four openness to experience inventories. *Journal of Personality*  
609 *Assessment, 101*(6), 574–588.

610 Christensen, A. P., Garrido, L. E., & Golino, H. (2021). Comparing community detection  
611 algorithms in psychological data: A monte carlo simulation. *PsyArXiv*.  
612 <https://doi.org/10.31234/osf.io/hz89e>

- 613 Christensen, A. P., Golino, H., & Silvia, P. J. (2019b). A psychometric network perspective  
614 on the measurement and assessment of personality traits. *Preprint*.
- 615 Christensen, A. P., Gross, G. M., Golino, H. F., Silvia, P. J., & Kwapil, T. R. (2019c).  
616 Exploratory graph analysis of the multidimensional schizotypy scale. *Schizophrenia*  
617 *Research, 206*, 43–51.
- 618 Cohen, J. (2013). *Statistical power analysis for the behavioral sciences*. Academic press.
- 619 Costantini, G., Richetin, J., Preti, E., Casini, E., Epskamp, S., & Perugini, M. (2019).  
620 Stability and variability of personality networks. A tutorial on recent developments in  
621 network psychometrics. *Personality and Individual Differences, 136*, 68–78.
- 622 Danon, L., Diaz-Guilera, A., Duch, J., & Arenas, A. (2005). Comparing community  
623 structure identification. *Journal of Statistical Mechanics: Theory and Experiment,*  
624 *2005(09)*, P09008.
- 625 Dijkstra, J. K., Cillessen, A. H., & Borch, C. (2013). Popularity and adolescent friendship  
626 networks: Selection and influence dynamics. *Developmental Psychology, 49(7)*, 1242.
- 627 Epskamp, S., Borsboom, D., & Fried, E. I. (2018). Estimating psychological networks and  
628 their accuracy: A tutorial paper. *Behavior Research Methods, 50(1)*, 195–212.
- 629 Epskamp, S., & Fried, E. I. (2018). A tutorial on regularized partial correlation networks.  
630 *Psychological Methods, 23(4)*, 617.
- 631 Feliciano, P., Daniels, A. M., Snyder, L. G., Beaumont, A., Camba, A., Esler, A., . . . others.  
632 (2018). SPARK: A us cohort of 50,000 families to accelerate autism research. *Neuron,*  
633 *97(3)*, 488–493.
- 634 Flores-Kanter, P. E., Garrido, L. E., Moretti, L. S., & Medrano, L. A. (2021). A modern  
635 network approach to revisiting the positive and negative affective schedule (panas)

- 636           construct validity.
- 637 Fortunato, S. (2010). Community detection in graphs. *Physics Reports*, *486*(3-5), 75–174.
- 638 Foygel, R., & Drton, M. (2010). Extended bayesian information criteria for gaussian  
639           graphical models. *arXiv Preprint arXiv:1011.6640*.
- 640 Friedman, J., Hastie, T., & Tibshirani, R. (2008). Sparse inverse covariance estimation with  
641           the graphical lasso. *Biostatistics*, *9*(3), 432–441.
- 642 Garrido, L. E., Abad, F. J., & Ponsoda, V. (2011). Performance of velicer’s minimum  
643           average partial factor retention method with categorical variables. *Educational and*  
644           *Psychological Measurement*, *71*(3), 551–570.
- 645 Garrido, L. E., Abad, F. J., & Ponsoda, V. (2013). A new look at horn’s parallel analysis  
646           with ordinal variables. *Psychological Methods*, *18*(4), 454.
- 647 Gates, K. M., Fisher, Z. F., Arizmendi, C., Henry, T. R., Duffy, K. A., & Mucha, P. J.  
648           (2019). Assessing the robustness of cluster solutions obtained from sparse count  
649           matrices. *Psychological Methods*.
- 650 Gates, K. M., Henry, T., Steinley, D., & Fair, D. A. (2016). A monte carlo evaluation of  
651           weighted community detection algorithms. *Frontiers in Neuroinformatics*, *10*, 45.
- 652 Gates, K. M., & Molenaar, P. C. (2012). Group search algorithm recovers effective  
653           connectivity maps for individuals in homogeneous and heterogeneous samples.  
654           *NeuroImage*, *63*(1), 310–319.
- 655 Girvan, M., & Newman, M. E. (2002). Community structure in social and biological  
656           networks. *Proceedings of the National Academy of Sciences*, *99*(12), 7821–7826.
- 657 Golino, H. F., & Epskamp, S. (2017). Exploratory graph analysis: A new approach for

- 658           estimating the number of dimensions in psychological research. *PloS One*, *12*(6).
- 659 Golino, H., Moulder, R., Shi, D., Christensen, A. P., Garrido, L. E., Nieto, M. D., . . . Boker,  
660           S. M. (2020). Entropy fit indices: New fit measures for assessing the structure and  
661           dimensionality of multiple latent variables. *Multivariate Behavioral Research*, 1–29.
- 662 Golino, H., Shi, D., Christensen, A. P., Garrido, L. E., Nieto, M. D., Sadana, R., . . .  
663           Martinez-Molina, A. (2020). Investigating the performance of exploratory graph  
664           analysis and traditional techniques to identify the number of latent factors: A  
665           simulation and tutorial. *Psychological Methods*.
- 666 Guttman, L. (1953). Image theory for the structure of quantitative variates. *Psychometrika*,  
667           *18*(4), 277–296.
- 668 Harman, H. H. (1976). *Modern factor analysis*. University of Chicago press.
- 669 Harris, C. W. (1962). Some rao-guttman relationships. *Psychometrika*, *27*(3), 247–263.
- 670 Hoffman, M., Steinley, D., Gates, K. M., Prinstein, M. J., & Brusco, M. J. (2018). Detecting  
671           clusters/communities in social networks. *Multivariate Behavioral Research*, *53*(1),  
672           57–73.
- 673 Hubert, L., & Arabie, P. (1985). Comparing partitions. *Journal of Classification*, *2*(1),  
674           193–218.
- 675 Lauritzen, S. L. (1996). *Graphical models* (Vol. 17). Clarendon Press.
- 676 Lubbe, D. (2019). Parallel analysis with categorical variables: Impact of category probability  
677           proportions on dimensionality assessment accuracy. *Psychological Methods*, *24*(3),  
678           339.
- 679 MacCallum, R. C., Widaman, K. F., Preacher, K. J., & Hong, S. (2001). Sample size in



- 680 factor analysis: The role of model error. *Multivariate Behavioral Research*, 36(4),  
681 611–637.
- 682 Marsman, M., Borsboom, D., Kruis, J., Epskamp, S., Bork, R. van, Waldorp, L., . . . Maris,  
683 G. (2018). An introduction to network psychometrics: Relating ising network models  
684 to item response theory models. *Multivariate Behavioral Research*, 53(1), 15–35.
- 685 Massara, G. P., Di Matteo, T., & Aste, T. (2016). Network filtering for big data:  
686 Triangulated maximally filtered graph. *Journal of Complex Networks*, 5(2), 161–178.
- 687 McNally, R. J. (2016). Can network analysis transform psychopathology? *Behaviour*  
688 *Research and Therapy*, 86, 95–104.
- 689 Montoya, A. K., & Edwards, M. C. (2020). The poor fit of model fit for selecting number of  
690 factors in exploratory factor analysis for scale evaluation. *Educational and*  
691 *Psychological Measurement*, 0013164420942899.
- 692 Newman, M. E. (2006). Modularity and community structure in networks. *Proceedings of*  
693 *the National Academy of Sciences*, 103(23), 8577–8582.
- 694 Orman, G. K., & Labatut, V. (2009). A comparison of community detection algorithms on  
695 artificial networks. In *International conference on discovery science* (pp. 242–256).  
696 Springer.
- 697 Pons, P., & Latapy, M. (2006). Computing communities in large networks using random  
698 walks. *J. Graph Algorithms Appl.*, 10(2), 191–218.
- 699 Schoemaker, M. M., Flapper, B., Verheij, N. P., Wilson, B. N., Reinders-Messelink, H. A., &  
700 Kloet, A. de. (2006). Evaluation of the developmental coordination disorder  
701 questionnaire as a screening instrument. *Developmental Medicine and Child*  
702 *Neurology*, 48(8), 668–673.

- 703 Steger, M. F. (2006). An illustration of issues in factor extraction and identification of  
704 dimensionality in psychological assessment data. *Journal of Personality Assessment*,  
705 *86*(3), 263–272.
- 706 Steinley, D. (2004). Properties of the hubert-arable adjusted rand index. *Psychological*  
707 *Methods*, *9*(3), 386.
- 708 Ward Jr, J. H. (1963). Hierarchical grouping to optimize an objective function. *Journal of*  
709 *the American Statistical Association*, *58*(301), 236–244.
- 710 Watanabe, H. (2001). Clustering as average entropy minimization and its application to  
711 structure analysis of complex systems. In "2001 iee international conference on  
712 systems, man and cybernetics": "E-systems and e-man for cybernetics in cyberspace"  
713 (Vol. 4, pp. 2408–2414). <https://doi.org/10.1109/ICSMC.2001.972918>
- 714 Watanabe, S. (1960). Information theoretical analysis of multivariate correlation. *IBM*  
715 *Journal of Research and Development*, *4*(1), 66–82.
- 716 Watson, D., Clark, L. A., & Tellegen, A. (1988). Development and validation of brief  
717 measures of positive and negative affect: The panas scales. *Journal of Personality*  
718 *and Social Psychology*, *54*(6), 1063.
- 719 Williams, D. R., Rhemtulla, M., Wysocki, A. C., & Rast, P. (2019). On nonregularized  
720 estimation of psychological networks. *Multivariate Behavioral Research*, *54*(5),  
721 719–750.
- 722 Yang, Z., Algesheimer, R., & Tessone, C. J. (2016). A comparative analysis of community  
723 detection algorithms on artificial networks. *Scientific Reports*, *6*, 30750.